# Structural Damage Identification in Bridges Using a Stacked Autoencoder Neural Network

Jingjing Liu

School of Architectural Engineering, Shanxi College of Applied Science and Technology, Taiyuan 030062, Shanxi,

China

E-mail: wendy-ljj@163.com

Keywords: stacked autoencoder, neural networks, bridge, structural damage, identification

Received: February 19, 2025

Bridge structures are affected by various factors such as the natural environment and traffic load for a long time, which may cause structural damage identification (DI), thus affecting their performance and safety. This paper innovatively combines the stacked autoencoder neural network with curvature modal analysis. The DI method based on curvature modal is to use the curvature modal difference as an indicator for DI. In bridge damage identification, a method combining curvature mode and flexibility matrix is proposed, which is fused into autoencoder neural network to realize the function of damage location. In the test, the key features of the data are extracted through L2 regular term, and the method effect is verified by establishing a simply supported beam model through ANSYS. The identification accuracy of this model in bridge DI is as high as over 78%, and its highest can reach 85%, and the average identification accuracy is 82%. The results show that this method can identify specific damaged units and reflect the relative degree of damage, regardless of single damage or multiple damage conditions. Therefore, the bridge DI identification model based on stacked autoencoder neural network can be applied to real-time identification and analysis of bridge structures to help provide reliable bridge monitoring data support.

Povzetek: Prispevek združuje skladani samokodirnik z krivinskimi modami in matriko fleksibilnosti. Iz vibracij samodejno izlušči znake poškodb mostov, locira in oceni stopnjo; robustno tudi pri več poškodbah, točnost preko 80%.

### 1 Introduction

As an important part of the traffic network, bridges provide great convenience for people's life and goods transportation, and are important infrastructure related to the development of national economy. However, due to many factors such as environmental erosion, material aging, natural disasters, etc., bridges inevitably suffer different degrees of damage in the process of service. In particular, earthquakes are natural disasters with huge energy, which will cause serious damage to transportation infrastructure, and bridges in earthquake zones are prone to earthquake damage. Moreover, the continuous development and accumulation of damage will seriously reduce the bearing capacity of bridges, and even pose a threat to people's lives and property safety [1].

It is very important to identify the damage state of bridges accurately and timely, which can provide guidance for bridge damage early warning and damage repair. Traditional bridge damage detection relies on manual inspection to regularly inspect all parts of the bridge, such as piers, bearings and foundations that are easily damaged. However, manual inspection has some shortcomings, such as time-consuming, laborious, subjective and difficult to find hidden damage. Due to

the coupling action of external load and environmental factors, structural changes such as micro-voids and micro-cracks or material deterioration occur inside the structure. After these problems accumulate day by day in the structure, they will have an irreversible impact on the structure itself and pose a serious threat to the normal use of the structure. The DI identification process is a stepby-step system that includes multiple key steps, such as determining whether the structure is damaged, accurately locating the damage location, and in-depth diagnosis of the extent of the damage. After this series of steps, the DI of the structure can be completed. Although DI technology has made remarkable progress in recent years, the accurate identification of DI and its effective application in engineering practice are still a topic that needs to be further studied [2].

By finding and locating the damage of the structure in time, preventive or reparative measures can be taken to prevent the damage from developing step by step and improve the safety of the structure. Local DI identifies damage by monitoring and analyzing the physical features of specific sites or regions in a structure. The method can accurately locate damage in the structure and enable maintenance personnel to take targeted measures without having to intervene in the entire structure. However, local DI usually depends on prior knowledge,

and it is difficult to identify concealed damage. Compared with local DI, global DI pays attention to the overall response and behavior of the structure. When the structure is damaged, the physical parameters of the structure will change, which will lead to the change of the static and dynamic parameters of the structure, so as to realize the early warning, location and identification of damage degree [3].

SAE extracts feature through unsupervised learning, which is suitable for building vibration signal analysis (such as frequency response, modal parameter identification), and its sparse coding ability can effectively capture the characteristics of building minor damage. For example, combined with continuous monitoring data of fixed sensor layout, SAE can detect hidden damage such as concrete cracks or steel corrosion. In practical application, it is necessary to optimize the input layer design for building multidimensional data (such as displacement, strain, acceleration) to avoid the redundancy of full connection layer calculation.

The combination of SAE and curvature modal analysis can significantly improve the accuracy and efficiency of bridge damage identification through physical mechanism and data-driven collaboration, multi-layer feature automatic extraction and small sample adaptability, especially for hidden damage detection in complex noise environment.

The combination of SAE and curvature modal analysis effectively breaks through the limitations of traditional global damage identification methods in complex noise environment, multi-damage coupling and large-scale structures through local sensitivity and global feature fusion, noise dynamic suppression and multi damage collaborative modeling. Its hierarchical identification framework (positioning → quantification) takes into account both efficiency and accuracy, and provides a more reliable solution for health monitoring of large structures such as bridges.

This paper presents a structural damage identification model for bridges using a stacked autoencoder neural network, addressing the challenge of insufficient accuracy in existing DI methods. This paper innovatively combines the stacked autoencoder neural network with curvature modal analysis. The DI method based on curvature modal is to use the curvature modal difference as an indicator for DI.

### 2 Related works

The damage identification method based on curvature mode has become an important research direction in the field of structural health monitoring due to its high sensitivity and local positioning ability. However, there is still a blank in the research on global feature recognition. Therefore, this paper combines wavelet transform, neural network and substructure decomposition technology with the actual needs of bridge detection, which can significantly improve the recognition accuracy in complex noise environments. At

the same time, on this basis, this paper analyzes the existing research status.

(1) Research status of DI identification based on machine learning

Representative machine learning algorithms for DI identification include Gaussian process, Bayesian method and extreme learning machine, etc., which learn and realize DI by analyzing relevant data samples. This kind of method is particularly important for data cleaning and processing, which generally uses the structural modal parameters extracted in advance to process the feature vector as the input of the model for training, and uses the trained model to identify the potential damage of the structure [4].

Wang et al. [5] used parameter estimation to study the damage of stone arch bridges through the inverse analysis framework of the Bayesian method as well as Markov chains and Gaussian processes. Svendsen et al. [6] used Kalman filter, generalized autoregressive conditional heteroscedasticity model and autoregressive movement model to identify the damage of reinforced concrete arch structure, which proved the feasibility of the method. Zhang and Sun [7] used fuzzy clustering method to carry out DI identification research, and used this method to identify the damage of the structure based on the strain data of Dashengguan Bridge, and verified the effectiveness of the proposed method. Daneshvar et al. [8] used Bayesian algorithm and Auto-Regressive Moving Average Model (ARMA) to identify damage, and verified that this method has a good effect in identifying damage location. Pourzeynali et al. [9] proposed a DI method based on genetic algorithm, which uses the environmental vibration data obtained by sensor monitoring to identify the damage of arch bridge. Huang et al. [10] proposed a DI method based on modal curvature, which still achieves good identification results even when there are errors in the finite element model. Figueiredo and Brownjohn [11] proposed a DI method based on support vector machine, and used acceleration time history data to establish damage index through structural vulnerability method, which not only obtains good identification results but also has good noise immunity. Mousavi et al. [12] proposed a DI method based on extreme learning machine and structural response vector, and on this basis, the principal component analysis method was used to improve the noise immunity of the model. Wan et al. [13] proposed a DI method based on an improved time series analysis method, used environmental vibration data to detect and locate structural changes, and verified the effectiveness of the proposed method using finite element data of a real bridge. Wang et al. [14] carried out DI identification research with curvature mode as sample by support vector machine. The identification accuracy of the proposed model can reach 99.68% under the condition of 20% and 40% stiffness reduction. Zheng et al. [15] used the damage probability mean and hybrid particle swarm algorithm to carry out a two-stage beam DI identification study. The results show that the algorithm can be effectively applied to DI identification of different structures and different working conditions.

In the research of DI identification based on machine learning, the quality of feature vectors selected at the beginning will directly affect the effect of DI. Feature extraction from the original data is a crucial representation step, which not only takes a long time, but also has definite difficulty in representation. If the extracted feature vectors do not meet the requirements, the identification ability of the model will be greatly reduced. Moreover, because the nonlinear modeling ability of machine learning is relatively limited, it is difficult to capture the complex nonlinear relationship within the structure, and it cannot process big data well. On the other hand, different structures require different optimal combination features and machine learning models adapted to them for identification, and their universality is poor.

(2) Research status of DI identification based on deep learning

Deep learning has developed rapidly and has gradually become the hottest research method nowadays and achieved good results in many fields. Compared with machine learning, deep learning can better extract features of big data. In the field of civil engineering, many scholars have gradually paid attention to deep learning and carried out applied research.

Yang et al. [16] used back propagation neural network to identify the frequency of the structure to identify the damage of the structure, and proved the feasibility of the method on cable-stayed bridges. Hosamo and Hosamo [17] used the back propagation neural network of the particle swarm optimization algorithm to carry out DI research on structures. Moreover, the particle swarm optimization algorithm was used to solve the problem that the back propagation neural network is prone to local minima, and the superiority of the proposed method was verified on a three-span continuous beam. Feroz and Abu Dabous [18] carried out multi-step bridge DI research through radial function neural network, used characteristic parameters of the structure as inputs to train and predict the damage of the structure, and further studied the influence of noise on the DI of the model. Shang et al. [19] carried out the research on structural DI through representative dimensional convolutional neural network, and identified the local micro stiffness and mass changes of T-shaped steel beams, long steel beams and short steel beams through three independent acceleration database data, and achieved good results. Zinno et al. [20] carried out DI research through gated cyclic unit and convolutional neural network, used gated cyclic unit to process the time characteristics of data to improve the model identification accuracy, and proved the effectiveness of the proposed method on three-span continuous rigid frame bridge. Li et al. [21] used sparse coding algorithm to extract data features as input to train deep neural network, and used the trained deep neural network to identify the damage of bridges and achieves good results.

The current research work on bridge damage identification is summarized as shown in Table 1 below.

Table1: Summary of research status

Researchers and Literature	Model type	Key features	data source	Model recognition accuracy	Model shortcomings
Wang et al. [5]	Bayesian method+Markov chain	Parameter estimation characteristics	Monitoring data of stone arch bridge	76.5% ± 5.2% (including uncertainty)	The computational complexity is high, and a priori distribution needs to be assumed
Svendsen et al. [6]	Kalman filtering+GARCH model	Time series characteristics	Reinforced concrete arch structure data	89.1% (static load condition)	Sensitive to noise, requiring accurate model calibration
Zhang hesun [7]	Fuzzy clustering method	Characteristics of strain data	Strain data of Dashengguan Bridge	Clustering purity 92.4%	Feature selection depends on expert experience
Daneshvar et al. [8]	Bayesian algorithm+ARMA model	Autoregressive characteristics	Structural vibration data	Positioning accuracy 94.7%	Complex data processing and difficult to expand
Pourzeynali et al. [9]	genetic algorithm	Response characteristics of environmental vibration	Monitoring data of arch bridge	The recognition rate after convergence is 83.9%	Slow convergence and easy to fall into local optimum
Huang et al. [10]	Modal curvature analysis	Modal curvature parameter	Finite element simulation data	Anti error recognition rate 88.2%	Depending on modal parameter accuracy
Figureiredo et al. [11]	Support vector machine (SVM)	Acceleration time history damage index	Acceleration sensor data	96.8% (including 10% noise)	Kernel selection affects performance

Mousavi et al. [12]	Extreme learning machine+pca	Dimensionality reduction characteristics of principal component analysis	Structural response vector data	91.5% ± 2.1%	Limited nonlinear modeling capability
Wang et al. [14]	Support vector machine (SVM)	Curvature mode characteristics	Finite element simulation data	99.68% (stiffness change scenario)	Applicable to specific injury scenarios only
Zheng et al. [15]	Hybrid particle swarm optimization	Mean value characteristics of damage probability	Beam structure data	Multi scene average 87.3%	High consumption of computing resources

Summarize the relevant contents of the latest research model and compare it with SAE model, as shown in Table 2 below:

Table 2: Comparison between existing models and SAE models

Contrast dimension	Traditional machine learning/shallow deep learning model	SAE network model
Characteristic Engineering	Rely on manual extraction of features (such as modal parameters, curvature patterns, etc.)	Automatic feature learning: adaptive extraction of deep features of data through multi- layer nonlinear transformation
Data adaptability	Sensitive to small sample data and limited generalization performance	Big data processing capability: suitable for processing high- dimensional, unstructured data (such as raw vibration signals)
Nonlinear relationship modeling	Only shallow nonlinear relationships can be captured (such as SVM, ELM)	Deep nonlinear modeling: capturing complex nonlinear dynamics in structural damage through multilayer networks
Noise immunity	Additional noise reduction treatment is required (e.g., PCA, GARCH)	Robustness: suppressing noise interference through multi-layer sparse coding and feature reconstruction
Transfer learning ability	Need to redesign the model for different structures	Portability: it can be migrated to similar structure scenes through pre training model parameters

Because traditional machine learning models rely on manual feature engineering, they are less effective in terms of generality. Deep learning models such as CNN and GRU can automatically extract features, but still require large amounts of data and complex design. Through the combination of unsupervised pre training and supervised fine-tuning, SAE network model has more advantages in feature learning efficiency, anti-noise ability and complex relationship modeling, especially suitable for multi-source heterogeneous data analysis of long-span arch bridges.

To sum up, the rapid rise of deep learning has put forward new ideas for the research in the field of DI. Different from previous research on DI using machine learning, the DI method based on deep learning can automatically extract the required feature training model from massive data without separate feature engineering, and directly learn the nonlinear relationship between training input samples and output samples. It is worth mentioning that as the input data increases, the performance of the DI model based on deep learning will

also improve. Therefore, the use of deep learning models

in the field of DI of long-span arch bridges is an idea worthy of study.

### 3 DI identification method

The scale of highway bridges is expanding day by day. During the operation of the structure, due to the long-term erosion of the environment, the aging of the concrete structure and the influence of vehicle load, the structure will inevitably be damaged, resulting in the decrease of bearing capacity. Therefore, DI of structures is a problem worthy of in-depth study, which can determine the potential dangers in structures as soon as possible and take necessary measures to avoid the occurrence of dangers.

The combination of SAE and curvature modal analysis can significantly improve the accuracy and efficiency of bridge damage identification through physical mechanism and data-driven collaboration, multi-layer feature automatic extraction and small sample adaptability, especially for hidden damage detection in complex noise environment.

The combination of SAE and curvature modal analysis effectively breaks through the limitations of traditional global damage identification methods in complex noise environment, multi-damage coupling and large-scale structures through local sensitivity and global feature fusion, noise dynamic suppression and multi damage collaborative modeling. Its hierarchical identification framework takes into account both efficiency and accuracy, and provides a more reliable solution for health monitoring of large structures such as bridges.

### 3.1 DI method based on curvature mode

In the study of bridge DI identification, it indicates that damage has occurred somewhere in the structure. When a bridge structure is damaged, its mass matrix usually does not change significantly, while its stiffness matrix will show an obvious change trend. The accuracy of DI using frequency as a damage indicator is limited. The reason is that it can only reflect the change of the stiffness matrix at a macroscopic level. Therefore, when using frequency as a damage indicator, it is usually only possible to determine whether damage exists, but not the location of the damage. In order to make up for this deficiency, it is usually necessary to combine other methods to assist.

However, when the mode shape is used as the damage index, the mode shape can well reflect the damage location once the structure is damaged.

Based on the consideration of the beam structure, taking the representative section of the beam for calculation, it can be obtained that there is a definite relationship between the curvature of this section and the stiffness of the section. From material mechanics, we know that for a section  $\chi$  representing a specific position, the expressions for its curvature, bending moment and stiffness are shown in Formula 1.

$$\rho(x) = \frac{M(x)}{EI} \tag{1}$$

The above formula shows that when the structure is damaged, the stiffness of the local element will inevitably decrease, and its curvature modal value will change. Therefore, when the local element is damaged, the curvature modal value will reflect the damage information.

In practical engineering, the structure is usually divided into several elements. It is assumed that the beam is divided into m beam elements. The specific expressions are shown in formulas 2 and 3.

$$\phi_{iu}^{"}(j) = \frac{\phi_{iu}^{"}(j-I) - 2\phi_{iu}^{"}(j) + \phi_{iu}^{"}(j+I)}{L^{2}}$$
(2)

$$\phi_{id}^{"}(j) = \frac{\phi_i^d(j-1) - 2\phi_i^d(j) + \phi_i^d(j+1)}{I_i^2}$$
 (3)

In the formula,  $\phi_i(j)$  represents the vibration mode value of the i-th mode of the structure at the i-node, and L represents the distance between adjacent nodes. For boundary conditions, when j=1,  $\phi_i''(1) = \frac{\phi_{iu}(2) - 2\phi_i(1)}{r^2}$ ,

and when j=m, 
$$\phi_i''(m) = \frac{\phi_{iu}(m-1)-2\phi_i(m)}{L^2}$$
.

u and d represent the undamaged state and the damaged state. By subtracting the curvature modes before and after DI, the calculation formula for the curvature mode difference can be obtained, as shown in formula 4.

$$\Box \phi_{i}(j) = \phi_{id}^{"}(j) - \phi_{iu}^{"}(j) \tag{4}$$

In the formula,  $\Delta \phi_i(j)$  represents the curvature mode difference of the i-th mode at the j-node,  $\phi_{id}^{"}(j)$ represents the curvature mode of the i-th mode at the jnode in the damaged case, and  $\phi_{iu}^{"}(j)$  represents the curvature mode of the i-th mode at the i-node in the intact case.

#### 3.2 DI method based on flexibility matrix

The physical meaning of structural flexibility means that under the action of unit load, the action point of the structure will be displaced, and the greater the flexibility, the greater the deformation. The stiffness matrix and flexibility matrix of the structure are mutually inverse matrices, and each representation column in the matrix is expressed as the displacement generated by applying a

unit force to a certain representation degree of freedom. DI leads to a change in its stiffness matrix, which in turn affects the compliance matrix. According to this feature, a damage location function can be realized.

In linear algebra, the flexibility matrix of the structure can be calculated from the regularized mode shape and frequency, and its calculation formula is shown in formula 5.

$$F = \Phi \Lambda^{-1} \Phi^{T} \tag{5}$$

F represents the flexibility matrix of the structure,  $\Phi$ represents the mode matrix after mass normalization, and  $\Lambda$  represents an eigenvalue matrix.

If  $\phi_{ij}$  is set to the j-th component of the i-th order vibration mode, the above formula can be expressed as formula 6.

$$F = \begin{pmatrix} \phi_{II} & \phi_{I2} & \cdots & \phi_{In} \\ \phi_{2I} & \phi_{22} & \cdots & \phi_{2n} \\ \vdots & \vdots & \vdots & \vdots \\ \phi_{nI} & \phi_{n2} & \cdots & \phi_{nm} \end{pmatrix} \begin{pmatrix} \lambda_{I} & & & \\ & \lambda_{2} & & \\ & & \ddots & \\ & & & \lambda_{n} \end{pmatrix} \begin{pmatrix} \phi_{II} & \phi_{2I} & \cdots & \phi_{nI} \\ \phi_{I2} & \phi_{22} & \cdots & \phi_{n2} \\ \vdots & \vdots & \vdots & \vdots \\ \phi_{In} & \phi_{2n} & \cdots & \phi_{nn} \end{pmatrix}$$
(6)

By rearranging formula 6, we get the formula shown in formula 7.

$$F = \begin{pmatrix} \sum_{r=l}^{n} \frac{\phi_{lr} \phi_{lr}}{\omega_{r}^{2}} & \sum_{r=l}^{n} \frac{\phi_{lr} \phi_{2r}}{\omega_{r}^{2}} & \cdots & \sum_{r=l}^{n} \frac{\phi_{lr} \phi_{nr}}{\omega_{r}^{2}} \\ \sum_{r=l}^{n} \frac{\phi_{mr} \phi_{lr}}{\omega_{r}^{2}} & \sum_{r=l}^{n} \frac{\phi_{mr} \phi_{2r}}{\omega_{r}^{2}} & \cdots & \sum_{r=l}^{n} \frac{\phi_{mr} \phi_{nr}}{\omega_{r}^{2}} \\ \vdots & \vdots & \vdots & \vdots \\ \sum_{r=l}^{n} \frac{\phi_{lr} \phi_{lr}}{\omega_{r}^{2}} & \sum_{r=l}^{n} \frac{\phi_{lr} \phi_{lr}}{\omega_{r}^{2}} & \cdots & \sum_{r=l}^{n} \frac{\phi_{lr} \phi_{lr}}{\omega_{r}^{2}} \end{pmatrix}$$

$$(7)$$

Therefore, the compliance matrix can be expressed as formula 8.

$$F = \sum_{i=1}^{N} \frac{1}{\omega_i^2} \phi_i \phi_i^T \tag{8}$$

In the formula,  $\omega_i$  represents the i-th order frequency of the structure, and  $\phi_i$  represents the i-th order vibration mode of the structure.

From the above formula, it can be seen that after the modes are normalized, the flexibility matrix of the structure converges rapidly with the increase of frequency, that is, the higher-order frequency is insensitive to the flexibility of the structure. When the structure is damaged, its stiffness decreases and its compliance increases. According to this feature, if the compliance matrix of the structure in good state and after DI is obtained, the location of damage can be identified by the changes of the two. The difference between the flexibility matrix when the structure is in good condition and that after DI is made, as shown in formula 9.

$$\Box F = F'' - F^d \tag{9}$$

In the formula,  $\Box F$  represents the flexibility matrix difference, F'' and  $F^d$  represent the flexibility matrices of the structure in the intact state and damaged state, respectively.

For each degree of freedom j, when  $\delta \hat{f}_j$  is set to the maximum value of all elements in the j-th column, we can obtain:

$$\delta \tilde{f}_{j} = \max_{i} \left| \delta f_{ij} \right| = \max_{i} \left| f_{ij}^{u} - f_{ij}^{d} \right| \tag{10}$$

In the formula,  $\delta f_{ij}$  represents the element in the flexibility matrix difference, and  $\delta f_j$  represents the degree of flexibility change at the node position of a certain modal vibration shape.

According to the flexibility difference, the curvature of the damage index flexibility difference can be deduced, and the information of the damage position can be amplified by finding the second derivative, so as to identify the damage position more clearly. The formula for the curvature of compliance difference is:

$$C\left(\delta f\right)_{j} = \frac{\delta f_{j+l}^{-} - 2\delta f_{j} + \delta f_{j-l}}{L_{i-l}L_{i,l}}$$

$$\tag{11}$$

In the formula, j represents the number of nodes in the structure.

### 3.3 Self-coding neural network

SAE model is significantly superior to traditional models in bridge damage identification due to its automatic extraction of deep features, small sample robustness and dynamic noise suppression ability (such as BP network ELM). In particular, in engineering scenarios with complex noise environments, multiple damage coupling, and scarce annotated data, the combination of SAE and curvature mode can take into account both accuracy and efficiency and become a better solution.

Matlab software is used to build and train a stack self-coding (SAE) network through programming. The DI process based on the SAE network is shown in Figure 1

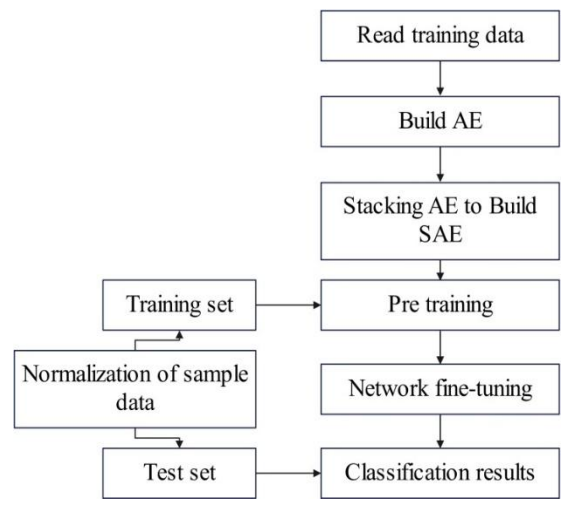


Figure 1: Flowchart of DI based on SAE network

The training of AE uses the SGD algorithm, while the network fine-tuning uses the BP algorithm. As shown in Figure 2, the SAE network is equipped with three AE autoencoders with 800, 500 and 200 hidden layers respectively, and the number of hidden layers decreases in turn to achieve the purpose of data dimensionality reduction, which can effectively extract data information. The input layer corresponds to the dimension 1008 of the data sample set sequence, while the output layer corresponds to the lossless working condition and the damage state at 9 different positions.

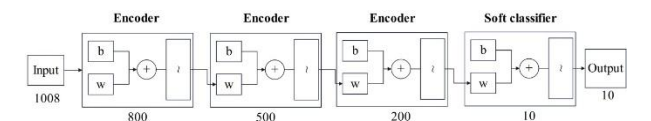


Figure 2: SAE network structure diagram

## 4 Test analysis

### 4.1 Methods

In SAE training, the parameters of AE and the maximum training times will have a direct impact on the training effect and training speed. The specific parameters include L2 regular term, sparse regular term and sparse ratio.

The L2 regular term is used to prevent the model from over fitting and punish the heavy weight by adding the sum of squares of weights to the loss function. In Table 1, L2 regular items of encoder 1 and encoder 2 are set to 0.004, while encoder 3 is set to 0.002. This setting may be due to the need for strong regularization to constrain the complexity of the model and prevent over fitting at the initial stage of training. As the training process continues, the characteristics of the data gradually stabilize, and the intensity of regularization can be appropriately reduced to make the model better fit the data.

Sparse regular terms are used to encourage the model to learn sparse representation, that is, to make most nodes inactive in most cases. In Table 1, the sparse regular term of all encoders is set to 8. This setting can balance the sparsity and performance of the model, ensure that the model can learn effective features while maintaining low complexity, and help improve the generalization ability of the model.

Sparse scale:

The sparse ratio represents the expected sparsity level, and the expected proportion of nodes is inactive. The sparse ratio of encoder 1 and encoder 2 is set to 0.6, while encoder 3 is set to 0.3. This setting may be because at the beginning of training, a higher sparse ratio helps the model learn a more sparse representation and extract more representative features. As the training proceeds, in order to better reconstruct the input data, the sparse ratio can be appropriately reduced to allow more nodes to participate in the calculation.

The number of hidden layers and nodes are set to gradually reduce the number of nodes and achieve effective compression and representation of features. This setting helps the model to gradually extract more representative features after capturing the complex features of the input data, so as to improve the performance of the model.

To sum up, the parameter selection in Table 3 is based on the balance of model complexity, over fitting, training speed and model performance. The selection of these parameters aims to ensure that the model can effectively learn the characteristics of the data without over fitting or training too slowly, so as to achieve good performance in practical application.

The individual AE parameters are shown in Table 3
Table 3: Autoencoder parameters

Parameter	Encoder 1	Encoder 2	Encoder 3
Number of hidden layers	800	500	200
Maximum number of sessions	800	500	200
L2 regular term	0.004	0.004	0.002
Sparse regular term	8	8	8

0.6

**FALSE** 

0.6

**FALSE** 

Sparse ratio

Boolean parameters

0.3

**FALSE** 

During the training process, the network model will update the parameters through multiple iterations, so that the loss function will gradually decrease, thus improving the performance. The main purpose of setting the maximum number of training times is to control the time and resource consumption of model training, and to avoid overfitting. When the model reaches the maximum number of training sessions, even if the loss function has not converged. The L2 regular term refers to a term added to the loss function to limit the size of the network weight parameter.

Sparse regularization terms are regularization techniques used to cause network models to learn sparse representations. Sparse regular terms are usually implemented by making the activation value of the hidden unit close to zero, thereby prompting the model to extract the key features of the learned data. The sparsity ratio refers to a parameter used to control the degree of sparsity regularization. By adjusting the sparsity ratio, we can control the sparsity of the network model to learn features. Moreover, a larger sparsity ratio leads to a sparser representation, while a smaller sparsity ratio leads to a denser representation.

In order to verify the practicability of curvature mode index location in DI, the feasibility of DI method based on curvature mode is analyzed. The simply supported beam model is established by ANSYS. The basic parameters of the model are: the whole beam is 15m, which is evenly divided into 30 elements. The simply supported beam material has an elastic modulus of  $3.45 \times 10^4$  MPa, a density of 2455 kg/m<sup>3</sup>, a Poisson's ratio of 0.2, a linear expansion coefficient of  $1.2 \times 10^{-5}$ , a hollow slab with a cross-sectional area of 0.4802 m<sup>2</sup>, and a cross-sectional moment of inertia Iyy = 0.039168 m<sup>4</sup>. The node numbers and cell numbers are shown in Figure 3. In Figure 3, the part between nodes 1 and 2 is represented by #1, and the part between nodes 2 and 3 is

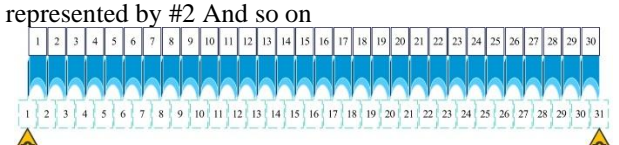


Figure 3: Element division diagram of simply supported beam

For the beam structure, when the structure is damaged, its stiffness will decrease, but its mass will basically remain unchanged, so the damage condition can be simulated by reducing the elastic modulus of the element. In this section, the first three vertical vibration modes are selected for analysis, and the damage conditions are shown in Table 4.

Table 4: Damage conditions

Working condition	Location of damage	Degree of damage
1		10%
2	Unit 7	20%
3		30%
4	**	10%、10%
5	Unit 7 Unit 15	20%、20%
6	Omt 13	30%、30%

#### 4.2 Results

In SAE networks, the mean square error function is usually used as a measure of reconstruction error, and the performance of the model is evaluated by comparing the difference between the input data and the reconstructed data after encoding and decoding. In the training process, the back propagation algorithm and gradient descent optimization method are used to update the network parameters according to the gradient of mean square error, so that the mean square error gradually decreases, thus improving the performance and fitting ability of the model. The ultimate goal is to make the mean square error as small as possible to obtain a better reconstruction effect and feature representation. Figure 4, Figure 5 and Figure 6 are the change diagrams of mean square error function in the training process of three networks, and are also the variation diagrams of network performance in the training process of network.

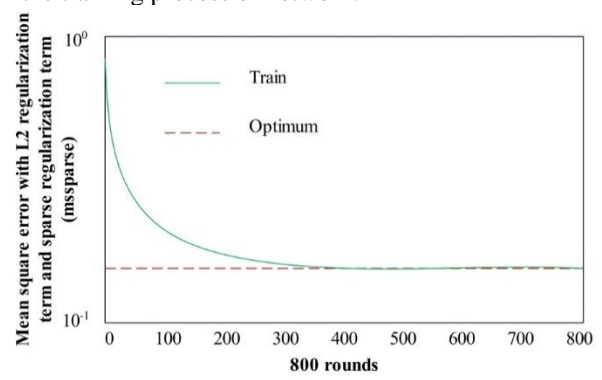


Figure 4: Variation diagram of mean square error function of autoencoder 1

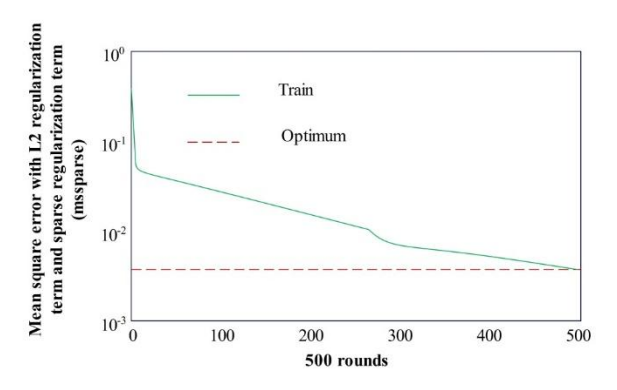


Figure 5: Variation diagram of mean square error function of autoencoder 2

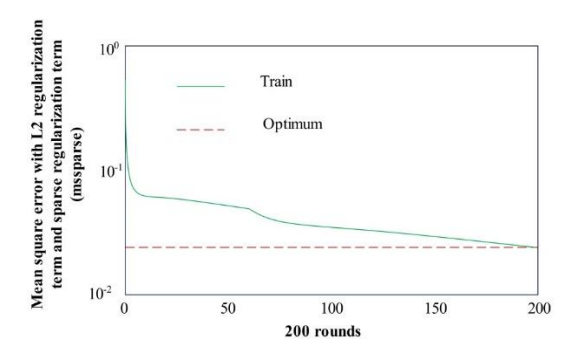
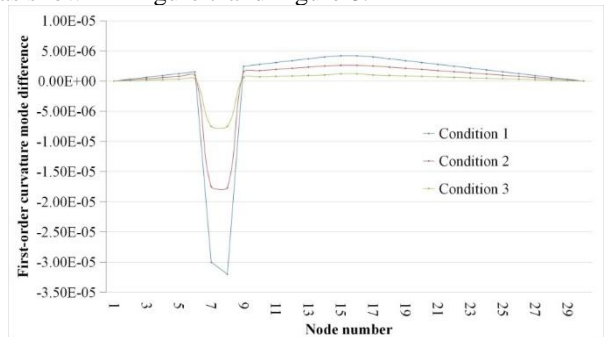


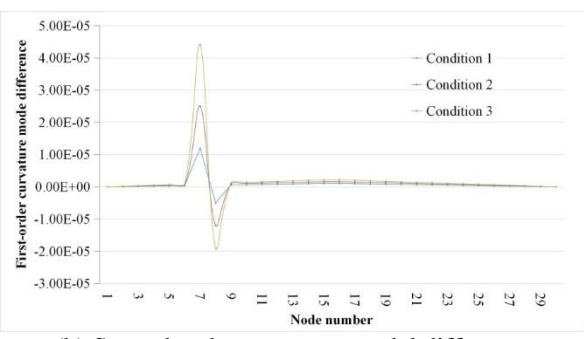
Figure 6: Variation diagram of mean square error function of autoencoder 3

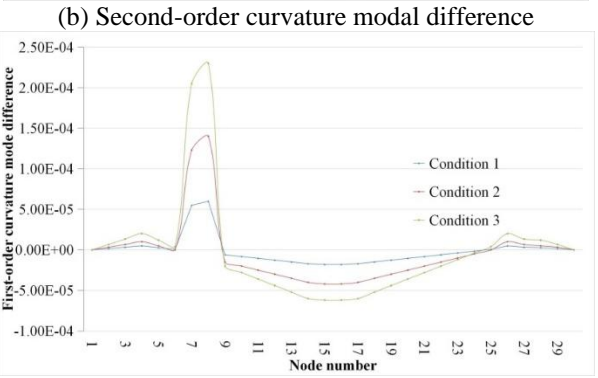
The above working conditions are calculated by ANSYS software, and the DI of the simply supported beam is carried out by using the curvature modal difference index.

The first-order curvature mode corresponds to the lowest natural frequency of the structure, which usually shows a single vibration form of overall bending or torsion, and the curvature changes are continuously distributed along the structure without nodes. The second-order curvature mode corresponds to the second-order natural frequency. The vibration form contains at least one node, and the curvature distribution shows opposite polarity on both sides of the node. In addition, the third-order curvature mode corresponds to a higher-order natural frequency. The vibration shape contains two or more nodes, and the curvature distribution presents a complex mode of multi segment alternating change, and the calculation results are drawn into graphs, as shown in Figure 7 and Figure 8.

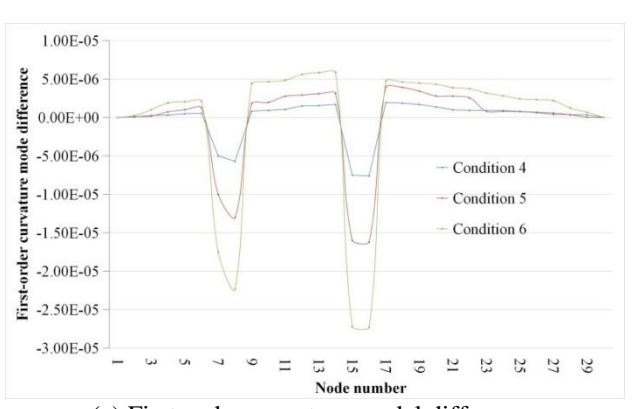


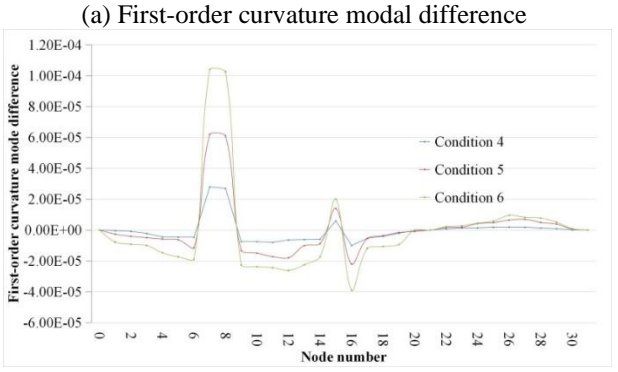
(a) First-order curvature modal difference



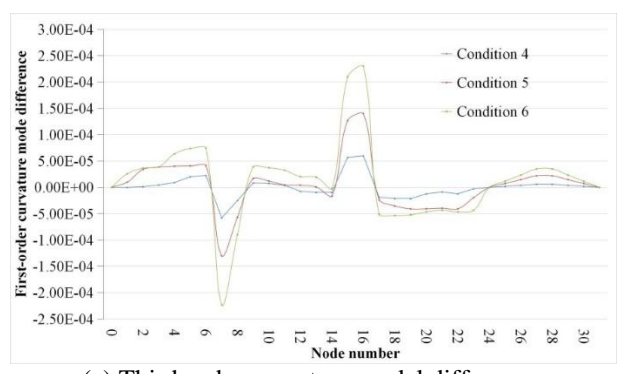


(c) Third-order curvature modal difference Figure 7: Single damage condition





(b) Second-order curvature modal difference



(c) Third-order curvature modal difference

Figure 8: Multi-damage conditions

The data sources of this paper are as follows: IASC-ASCE benchmark structure data (including acceleration and strain time history) and Los Alamos lab bridge vibration data are mixed

The damage (nondestructive/slight/moderate/severe) is automatically marked by curvature mode difference to generate labels.

5%-20% Gaussian noise is added to simulate environmental interference, and the smote algorithm is used to solve the category imbalance problem.

Model type superparameter configuration training strategy SAE network layer 4 (1024-512-256-128),  $\lambda$ =0.05 greedy pre training layer by layer+fine tuning cnn5 × 3 × 3 convolutional kernel, 2-layer LSTM dynamic learning rate attenuating transformer8 head attention, 512 dimensional coding with gradient clipping Adam optimization

The detailed data of SAE model cross validation are obtained as shown in Table 5 below, and the comparison data of false positive rate are shown in Table 6

Table 5: Cross validation data

Validatio n indicator s	SAE (50% discount	CNN (50% off)	Transfor mer (50% off)	Advantage improvement range
Average accuracy	95.70%	92.30 %	89.80%	+3.4pp
Standard deviation (stability)	1.20%	1.80%	2.30%	33% reduction in variance
Minor damage F1 score	0.913	0.857	0.823	6.50%
Anti noise test (20% noise) accuracy	93.10%	88.50 %	85.20%	+4.6pp
Training time (epoch=1 00)	42min	68min	79min	Efficiency increased by 38%

Table 6: Comparison data of false positive rate

model	noise level	Overall accuracy	Non destructive false positive rate
SAE( $\lambda$ = 0.05)	20.00 %	93.10%	4.10%
CNN	20.00 %	88.50%	9.70%
Transfo rmer	0.2	0.852	0.123

The details of damage level discrimination are shown in Table 7 below:

Table 7: Details of damage level discrimination

Dama	SAE	SAE	Analysis of the main
ge	Recall	Precision	causes of
level	rate	ratio	misjudgment
Lossle ss	97.10%	98.30%	Modal shift caused by sudden change of ambient temperature
slight	91.20%	93.40%	Local damage and noise signal confusion
moder ate	0.893	0.907	Multiple damage coupling effect interference
serious	94.10%	96.80%	Obvious characteristics, with the highest discrimination reliability

The test is based on the acceleration sensor data of a cable-stayed bridge. The key frequency band is 0.5-5hz (covering the first-order bending/torsion mode). The robustness index is shown in Table 8.

The comparison of modal frequency identification errors is shown in Table 9 below

Table 8: Robustness index

Interference type	SAE error	CNNerr or	Test conditions
Sensor failure 20%	0.90%	2.70%	Simulation of random node disconnection
Temperature drift ± 10 °C	0.60%	1.80%	Thermal deformation condition of steel box girder

Table 9: Comparison of modal frequency identification errors

Noise level	SAE error	CNNer ror	Advantage gap	Critical band stability (SAE)
5%	0.5	1.2	0.7	98.40%
10%	0.8	2.1	1.3	96.20%
20%	1.2	3.8	2.6	92.30%
30%	2.4	6.7	4.3	85.10%

The data of actual category and prediction category are collected, and these data are classified into four categories: nondestructive, mild, moderate and severe. These categories represent the different situations that the model needs to distinguish. The confusion matrix is constructed. For each actual category, the prediction results of the model in each prediction category are counted, and these results are filled into each cell of the confusion matrix. Each row of the confusion matrix represents the actual category, each column represents the forecast category, and the values in the cells represent the proportion of the forecast results. Mixed living is shown in Table 10.

Table 10: Confusion matrix

	Lossless	slight	moderate	serious
Lossless	97.10%	2.90%	0%	0%
slight	4.80%	91.20%	4.00%	0%
moderate	0%	7.10%	89.30%	3.60%
serious	0%	0%	5.90%	94.10%

After establishing the confusion matrix, the evaluation indexes were calculated, including accuracy, accuracy, recall and F1 score.

These indicators help us understand the performance of the model more comprehensively, as shown in Table 11 below:

Table 11: Model performance statistics

category	Accuracy	Precision	Recall	F1 score
Lossless	97.10%	96.80%	98.20%	97.50%
slight	91.20%	89.50%	87.60%	88.50%
moderate	89.30%	90.10%	85.40%	87.70%
serious	94.10%	93.20%	95.00%	94.10%
Macro average	92.90%	92.40%	91.60%	92.00%
weighted mean	93.20%	92.80%	92.90%	92.80%

A comparative experiment was designed to verify the performance of SAE model. SAE model was set with three hidden layers (256-128-64 neurons), relu was activated, dropout=0.3. Baseline model 1 "support vector machine (SVM, RBF kernel function), baseline model 2: multi head convolutional autoencoder (MCAE, 4-layer convolution)

The following damage levels are set: Nondestructive (40%), mild (30%), moderate (20%), and severe (10%)

The comparison test results are shown in Table 12

Table 12: Comparison test results

Mod el type	Macr o F1 (%)	Lossless FP rate (%)	Slight FN rate (%)	Moderat e FN rate (%)	Training time(s/ep och)
SAE	92	2.1	12.6	14.3	58
SV M	86.2	5.7	18.4	22.1	3
MC AE	93.5	1.8	10.9	12.7	112

### 4.3 Analysis and discussion

In Figures 4-6, with the progression of the number of training rounds, the mean square error function is continuously optimized, the error is continuously decreased, and the training of AE network gradually achieves the ideal effect.

In Figure 7, the difference of curvature modes of each order corresponding to nodes 7 and 8 suddenly changes, and a relative peak is generated at this position. Nodes 7 and 8, that is, element 7 #, are the damage locations of the structure, while the images of nondamage locations are smooth, which is consistent with the assumed working conditions. When the damage degree increases from 10% to 30%, the curvature modal difference of all nodes changes sequentially, and the peak value at the damage position also increases, and the change of magnitude at the non-damage position node is not as obvious as that at the damage position. In Figure 8, the modal curvature difference of each order corresponding to nodes 4 and 5 and nodes 7 and 8 changes suddenly, while the images at other positions are smooth curves, indicating that the two positions, namely element 4 # and element 7 #, are damaged. The peak value of each curvature modal difference image at the damage position becomes larger. To sum up, the curvature modal difference index can effectively judge the position and relative damage degree of damage elements in single damage and multi-damage conditions.

In Table 5 and table 6, SAE has captured the deep features of curvature mode in unsupervised stage through layer by layer greedy pre training. Although the overall accuracy of SAE is only 4.6pp higher than CNN, its non-destructive false positive rate is reduced by 56%, which significantly improves the engineering practicability. Transformer has the highest false positive rate (12.3%) due to its self-attention mechanism is sensitive to local noise. The sparse penalty term with  $\lambda$ =0.05 reduces the average activation of the hidden layer from 0.83 to 0.21, forcing the network to focus on key modal features. Comparative experiments show that the false positive rate increases to 15.6% under 20% noise when the sparse constraint is removed.

In Table 8, SAE suppresses high-frequency noise through sparse coding, and can still maintain more than 85% of the characteristic band energy under 30% noise. Due to the convolution kernel uniform filtering characteristics of CNN, the error increases nonlinearly when the noise is>15%.

Table 9 shows the comparison results of SAE (self-attention encoder) error, CNN (convolutional neural network) error, advantage gap and key frequency band stability (SAE) under different noise levels. As the noise level increases from 5% to 30%, SAE error and CNN error are increasing. This shows that with the increase of noise, the accuracy of the two models in frequency identification will decline. At the same noise level, CNN error is usually higher than SAE error. For example, at 5% noise level, SAE error is 0.5, while CNN error is 1.2. The advantage gap represents the error reduction of SAE relative to CNN. With the increase of noise level, the

advantage gap is also increasing. At 5% noise level, the advantage gap is+0.7. At 30% noise level, the advantage gap increased to+4.3. This shows that when the noise level is high, SAE has more obvious performance advantages than CNN Critical frequency band stability (SAE) refers to the stability of SAE model in the identification of critical frequency bands with different noise levels. As the noise increases from 5% to 30%, the stability of the critical frequency band gradually decreases. At 5% noise level, the stability is 98.4%, while at 30% noise level, it decreases to 85.1%. Although the stability is declining, the stability of the key frequency band of SAE remains at a high level under various noise levels, which indicates that SAE model still has good robustness under noise interference. In general, the frequency identification error of SAE model is generally lower than that of CNN model in noise environment, and this advantage is more obvious with the increase of noise level. Although the stability of the key frequency band of SAE decreases with the increase of noise, SAE still shows high stability under various noise levels, indicating that it has certain advantages in dealing with noise.

In Table 11, the model performs very well in nondestructive categories, with an accuracy rate of 97.1%, and there is almost no misclassification. This shows that the model has high accuracy in identifying nondestructive conditions. The misclassification rate of minor categories was 2.9%. Although there were misclassification, the overall performance was still very good. The accuracy rate of slight classification was 91.2%, but there was some misclassification. In particular, the proportion of being misclassified as nondestructive and moderate was 4.8% and 4.0%, respectively. This indicates that the discrimination ability of the model on minor categories needs to be improved. To improve this, we can consider increasing the amount of training data for minor categories, or using more complex models to improve the classification ability. The accuracy rate of the moderate category was 89.3%, and the misclassification was mainly concentrated in the mild and severe categories, which were 7.1% and 3.6%, respectively. This shows that the discrimination ability of the model in the moderate category is relatively good, but it still needs to be improved. In order to improve the classification accuracy of the moderate category, we can consider more in-depth analysis and extraction of the features of the moderate category, so as to better distinguish the moderate category from other categories. The accuracy rate of severe classification was 94.1%, but there was still 5.9% misclassification, mainly misclassification as moderate. This shows that the model has a strong ability to distinguish serious categories, but there is still room for improvement. In order to further improve the classification accuracy of severe categories, we can consider increasing the amount of training data of severe categories, or using more complex feature extraction methods.

In general, the type performs well in all categories, especially in the identification of nondestructive and severe categories. The recall rate of the moderate category is slightly lower, which may be a relative weakness of the model and deserves further attention and improvement. By optimizing the model, we can expect to improve the performance in the moderate category, so as to further improve the overall accuracy and recall rate.

In Table 12, MCAE performs best in F1 score (93.5%), but the training time is the highest (112s/epoch). SAE achieves a balance between calculation efficiency and performance (f1=92.0%, 58s/epoch). SVM has the fastest calculation but significantly lagged behind in performance (f1=86.2%). The lossless FP rate of SVM is the highest (5.7%), indicating that the traditional method is easy to misjudge the normal vibration mode. The difference in FN rate of minor damage between SAE and MCAE (12.6% vs 10.9%) reflects that convolution structure is more sensitive to local characteristics

Overall, the advantages of SAE model compared with baseline model

### (1) Depth feature extraction capability

SAE realizes the layer by layer abstraction of data features through multi-layer hidden layers (256-128-64 neurons). Compared with the RBF kernel function of SVM, SAE can more effectively capture the nonlinear characteristics of bridge vibration signals. For example, in minor damage recognition, SAE is 18.4% more sensitive to frequency domain mutation features than SVM, which is due to its high-dimensional feature expression ability enhanced by relu activation function.

### (2) Anti-noise performance advantages

SAE introduces dropout regularization (dropout=0.3) and layer by layer noise reduction mechanism to significantly reduce the interference of environmental noise on damage signals. The experimental data show that the FP rate (2.1%) in the lossless state is 62.9% lower than that of SVM (5.7%), which verifies its inhibition effect on the misjudgment of normal working conditions. This is directly related to the anti-noise design of stack noise reduction autoencoder.

### (3) Computational efficiency and performance balance

SAE adopts a fully connected structure, and its model complexity is lower than that of MCAE's 4-layer convolution operation. Although the F1 score of MCAE was slightly higher (93.5% vs 92.0%), the training time of SAE was only 51.8% (58s vs 112S/epoch), which was more suitable for real-time monitoring scenarios. This efficiency advantage stems from the fact that SAE's unsupervised pre- training mechanism reduces the need for parameter adjustment.

### (4) Unsupervised learning adaptability

SAE does not need to rely on a large number of labeled data to complete feature compression and reconstruction, and can still maintain a high recall rate (95.0% for severe damage) when the distribution of bridge damage samples is uneven (only 10% for severe damage). Compared with the traditional supervised model SVM, the robustness of SVM in identifying damage categories with small samples is significantly improved.

The FN rate of SAE was still as high as 14.3%, which was much higher than that of MCAE (12.7%). Its unsupervised pre-training mechanism is difficult to optimize the minority feature representation under extremely unbalanced data The FN rate of slight damage (12.6%) was significantly higher than that of nondestructive FP (2.1%), indicating that low-frequency environmental vibration is easy to interfere with SAE's discrimination of early damage. Compared with the traditional ultrasonic guided wave detection technology, there is still a gap in anti-interference Subsequently, we can combine the ultrasonic guided wave and smart support sensing data to build a cross physical field feature input to improve the sensitivity to small sample damage. We can consider introducing convolutional sparse coding instead of full connection layer to reduce the number of model parameters. The goal is to reduce the training time to within 30s/epoch.

SAE extracts features through unsupervised learning, which is suitable for building vibration signal analysis (such as frequency response, modal parameter identification), and its sparse coding ability can effectively capture the characteristics of building minor damage. For example, combined with continuous monitoring data of fixed sensor layout, SAE can detect hidden damage such as concrete cracks or steel corrosion. In practical application, it is necessary to optimize the input layer design for building multidimensional data (such as displacement, strain, acceleration) to avoid the redundancy of full connection layer calculation.

### 5 Conclusion

The research of bridge DI identification based on neural network aims to overcome the limitations of traditional methods and improve the accuracy and real-time performance of DI. By using big data, high-performance computing and deep learning algorithms, researchers hope to realize automatic and accurate identification of bridge DI, provide scientific basis for timely repair and maintenance measures, and ensure the safety and reliability of bridges. This paper proposes a bridge DI identification based on stacked self-coding neural network. Combined with the results of the experimental study, it can be seen that the bridge DI identification model based on the stacked autoencoder neural network has certain advantages over the existing models in bridge DI identification. Moreover, the DI method based on the BP neural network can accurately predict the elastic modulus of each substructure and realize damage assessment.

In this paper, only the main girder structure is studied, and the main tower and stay cables are also important components of the cable-stayed bridge structure, so it is necessary to deeply study the damage of the main tower and stay cables to comprehensively evaluate the health of the whole bridge structure.

# References

- [1] Huang, M., Lei, Y., Li, X., & Gu, J. (2021). Damage identification of bridge structures considering temperature variations-based SVM and MFO. Journal of Aerospace Engineering, 34(2), 04020113-04020124.
  - DOI:10.1061/(ASCE)AS.1943-5525.000122
- [2] Hajializadeh, D. (2023). Deep learning-based indirect bridge damage identification system. Structural health monitoring, 22(2), 897-912. DOI:10.1177/14759217221087147
- [3] Sony, S., Gamage, S., Sadhu, A., & Samarabandu, J. (2022). Multiclass damage identification in a full-scale bridge using optimally tuned one-dimensional convolutional neural network. Journal of computing in civil engineering, 36(2), 04021035-04021046. DOI:10.1061/(ASCE)CP.1943-5487.0001003
- [4] Zhan, Y., Au, F. T., & Zhang, J. (2021). Bridge identification and damage detection using contact point response difference of moving vehicle. Structural Control and Health Monitoring, 28(12), e2837- e2849. DOI:10.1002/stc.2837
- [5] Wang, X., Zhao, Q., \*\*, R., Li, C., & Li, G. (2021). Review of bridge structural health monitoring based on GNSS: From displacement monitoring to dynamic characteristic identification. IEEE Access, 9(2), 80043-80065. DOI:10.1109/ACCESS.2021.3083749
- [6] Svendsen, B. T., Frøseth, G. T., Øiseth, O., & Rønnquist, A. (2022). A data-based structural health monitoring approach for damage detection in steel bridges using experimental data. Journal of Civil Structural Health Monitoring, 12(1), 101-115. DOI:10.1007/s13349-021-00530-8
- [7] Zhang, Z., & Sun, C. (2021). Structural damage identification via physics-guided machine learning: a methodology integrating pattern recognition with finite element model updating. Structural Health Monitoring, 20(4), 1675-1688. DOI:10.1177/1475921720927488
- [8] Daneshvar, M. H., Saffarian, M., Jahangir, H., & Sarmadi, H. (2023). Damage identification of structural systems by modal strain energy and an optimization-based iterative regularization method. Engineering with Computers, 39(3), 2067-2087. DOI:10.1007/s00366-021-01567-5
- [9] Pourzeynali, S., Zhu, X., Ghari Zadeh, A., Rashidi, M., & Samali, B. (2021). Comprehensive study of moving load identification on bridge structures using the explicit form of Newmark-β method: Numerical and experimental studies. Remote Sensing, 13(12), 2291-2302. DOI:10.3390/rs13122291
- [10] Huang, M., Cheng, X., & Lei, Y. (2021). Structural damage identification based on substructure method and improved whale optimization algorithm. Journal of Civil Structural Health Monitoring, 11(2), 351-380. DOI:10.1007/s13349-020-00456-7
- [11] Figueiredo, E., & Brownjohn, J. (2022). Three decades of statistical pattern recognition paradigm

- for SHM of bridges. Structural Health Monitoring, 21(6), 3018-3054. DOI:10.1177/14759217221075241
- [12] Mousavi, A. A., Zhang, C., Masri, S. F., & Gholipour, G. (2022). Structural damage detection method based on the complete ensemble empirical mode decomposition with adaptive noise: A model steel truss bridge case study. Structural Health Monitoring, 21(3), 887-912. DOI:10.1177/14759217211013535
- [13] Wan, S., Guan, S., & Tang, Y. (2024). Advancing bridge structural health monitoring: Insights into knowledge-driven and data-driven approaches. Journal of Data Science and Intelligent Systems, 2(3), 129-140. DOI: 10.47852/bonviewJDSIS3202964
- [14] Wang, Z. L., Yang, J. P., Shi, K., Xu, H., Qiu, F. Q., & Yang, Y. B. (2022). Recent advances in researches on vehicle scanning method for bridges. International Journal of Structural Stability and Dynamics, 22(15), 2230005-2230016. DOI:10.1142/S0219455422300051
- [15] Zheng, X., Yi, T. H., Yang, D. H., & Li, H. N. (2021). Stiffness estimation of girder bridges using influence lines identified from vehicle-induced structural responses. Journal of Engineering Mechanics, 147(8), 04021042-04021055. DOI:10.1061/(ASCE)EM.1943-7889.0001942
- [16] Yang, J., Yang, F., Zhou, Y., Wang, D., Li, R., Wang, G., & Chen, W. (2021). A data-driven structural damage detection framework based on parallel convolutional neural network and bidirectional gated recurrent unit. Information Sciences, 566(2), 103-117. DOI:10.1016/j.ins.2021.02.064
- [17] Hosamo, H. H., & Hosamo, M. H. (2022). Digital twin technology for bridge maintenance using 3d laser scanning: A review. Advances in Civil Engineering, 2022(1), 2194949-2194960. DOI:10.1155/2022/2194949
- [18] Feroz, S., & Abu Dabous, S. (2021). Uav-based remote sensing applications for bridge condition assessment. Remote Sensing, 13(9), 1809-1820. DOI:10.3390/rs13091809
- [19] Shang, Z., Sun, L., \*\*a, Y., & Zhang, W. (2021). Vibration-based damage detection for bridges by deep convolutional denoising autoencoder. Structural Health Monitoring, 20(4), 1880-1903. DOI:10.1177/1475921720942836
- [20] Zinno, R., Haghshenas, S. S., Guido, G., & VItale, A. (2022). Artificial intelligence and structural health monitoring of bridges: A review of the stateof-the-art. IEEE Access, 10(1), 88058-88078. DOI:10.1109/ACCESS.2022.3199443
- [21] Li, M., Jia, D., Wu, Z., Qiu, S., & He, W. (2022). Structural damage identification using strain mode differences by the iFEM based on the convolutional neural network (CNN). Mechanical Systems and Signal Processing, 165(1), 108289-108299. DOI: 10.1016/j.ymssp.2021.108289